Correction

NEUROSCIENCE

Correction for "Genetic rescue models refute nonautonomous rod cell death in retinitis pigmentosa," by Susanne F. Koch, Jimmy K. Duong, Chun-Wei Hsu, Yi-Ting Tsai, Chyuan-Sheng Lin, Christian A. Wahl-Schott, and Stephen H. Tsang, which appeared in issue 20, May 16, 2017, of *Proc Natl Acad Sci USA* (114:5259–5264; first published May 3, 2017; 10.1073/pnas.1615394114).

The authors note that Fig. 3 appeared incorrectly. The corrected figure and its legend appear below.

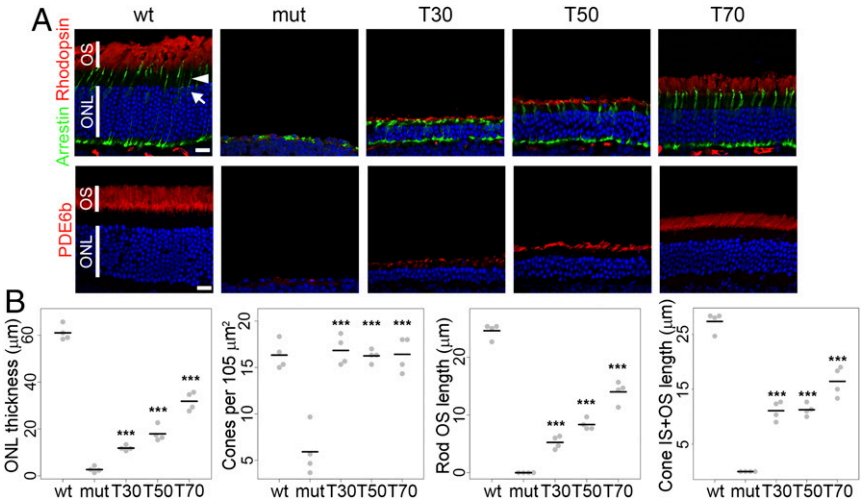

Fig. 3. Restoration of PDE6b expression rescues rods and partially restores OS length, in a dose-dependent fashion, and prevents cone death. *Pde6b*^{STOP}/*Pde6b*^{H620Q}, *Pde6g::CreERT2* mice were injected with 25, 50, or 100 μg/g BW tamoxifen to rescue 30% (T30), 50% (T50), or 70% (T70) of rods, respectively; untreated mutants (mut) and wild-type mice (*Pde6b*$^{+}$/*Pde6b*^{H620Q}, *Pde6g::CreERT2*, WT) were not injected. Tamoxifen injections were in 1-mo-old mice; at 9 mo of age, retinas were sectioned and immunolabeled. (*A*) Antibodies: rhodopsin or PDE6b (rod OSs, red) and arrestin (cones, green). Hoechst dye, nuclei, blue. Arrows, arrestin-immunopositive cone cell bodies; arrowheads, arrestin-immunopositive cone OSs. (*B*) Rhodopsin and arrestin immunolabeled sections were quantitatively analyzed for ONL thickness, cone number, rod OS length and cone IS + OS length. Gray dots, individual mice ($n = 4$ for each group); horizontal black lines, group means. Treated and untreated groups were compared by a linear regression model: ***$P < 0.001$. IS, inner segment; ONL, outer nuclear layer; OS, outer segment. (Scale bar, 15 μm.)

www.pnas.org/cgi/doi/10.1073/pnas.1708940114

Genetic rescue models refute nonautonomous rod cell death in retinitis pigmentosa

Susanne F. Koch[a,b,c], Jimmy K. Duong[d], Chun-Wei Hsu[a,b,c], Yi-Ting Tsai[a,b,c,e], Chyuan-Sheng Lin[f], Christian A. Wahl-Schott[g], and Stephen H. Tsang[a,b,c,d,f,1]

[a]Jonas Children's Vision Care, Departments of Ophthalmology, Pathology, and Cell Biology, Columbia University, New York, NY 10032; [b]Bernard & Shirlee Brown Glaucoma Laboratory, Departments of Ophthalmology, Pathology, and Cell Biology, Columbia University, New York, NY 10032; [c]Edward S. Harkness Eye Institute, New York Presbyterian Hospital, New York, NY 10032; [d]Department of Biostatistics, Mailman School of Public Health, Columbia University Medical Center, New York, NY 10032; [e]Institute of Human Nutrition, College of Physicians and Surgeons, Columbia University, New York, NY 10032; [f]Herbert Irving Comprehensive Cancer Center, Columbia University Medical Center, New York, NY 10032; and [g]Center for Integrated Protein Science Munich (CIPSM) at the Department of Pharmacy–Center for Drug Research, Ludwig-Maximilians-Universität München, 81377 Munich, Germany

Edited by Roderick R. McInnes, Lady Davis Institute, McGill University, Montreal, Canada, and accepted by Editorial Board Member Jeremy Nathans April 7, 2017 (received for review September 14, 2016)

Retinitis pigmentosa (RP) is an inherited neurodegenerative disease, in which the death of mutant rod photoreceptors leads secondarily to the non-cell autonomous death of cone photoreceptors. Gene therapy is a promising treatment strategy. Unfortunately, current methods of gene delivery treat only a fraction of diseased cells, yielding retinas that are a mosaic of treated and untreated rods, as well as cones. In this study, we created two RP mouse models to test whether dying, untreated rods negatively impact treated, rescued rods. In one model, treated and untreated rods were segregated. In the second model, treated and untreated rods were diffusely intermixed, and their ratio was controlled to achieve low-, medium-, or high-efficiency rescue. Analysis of these mosaic retinas demonstrated that rescued rods (and cones) survive, even when they are greatly outnumbered by dying photoreceptors. On the other hand, the rescued photoreceptors did exhibit long-term defects in their outer segments (OSs), which were less severe when more photoreceptors were treated. In summary, our study suggests that even low-efficiency gene therapy may achieve stable survival of rescued photoreceptors in RP patients, albeit with OS dysgenesis.

neurodegeneration | retinitis pigmentosa | photoreceptor cell death | non-cell autonomous degeneration | gene therapy

Retinitis pigmentosa (RP) is a group of retinal degenerative diseases and the most common cause of inherited blindness (1). Most often, RP results from mutations in rod-specific genes, which trigger the cell-autonomous loss of rods that, in turn, causes the non-cell autonomous loss of cones (2). Gene therapy strategies are being intensively developed and tested for RP and other inherited retinal degenerative diseases. However, the barriers to developing a successful gene therapy are significant. For example, current methods of gene delivery (in both humans and mice) transduce only a fraction of the diseased cells. In retinas, the result is a mosaic of treated/rescued rods (and cones), surrounded by large numbers of untreated/diseased rods. Here, we tested whether untreated dying rods impact survival, structure, and/or function of treated rods. In addition, we set out to examine the non-cell autonomous effects of dying rods on cones in greater detail. To do this, we generated mice in which the photoreceptor layer is a mosaic of treated and untreated mutant rods and rescue is spatially or numerically controlled. In these mice, the mutant rods lack the gene encoding rod-specific cGMP phosphodiesterase 6b (*Pde6b*)—a common cause of autosomal recessive RP (3). Analysis of our mosaic retinas revealed that untreated dying rods did not impact survival of rescued rods or cones but did trigger outer segment (OS) dysgenesis in nearby rods and cones, which persisted after the mutant rods have all died.

Results

Cre-Driven Gene Rescue Produces Mosaic Retinas in Which the Ratio of Mutant and Wild-Type Photoreceptors Is Controlled. To investigate the fate of rescued rods in a pathological environment, we used two different strategies. For both, we created RP mice whose retinal photoreceptor layer is a mosaic of treated and untreated rods—as well as cones. In one strategy, treated and untreated rods were spatially segregated; in the second, they were diffusely intermixed, and the percentage of rescued rods was controlled. For both models, we used our genetically engineered RP mouse model $Pde6b^{STOP}/Pde6b^{H620Q}$, in which one allele of rod-specific *Pde6b* contains a point mutation and the second allele a floxed STOP cassette. In these mice, PDE6b is dramatically reduced, leading to rod death and secondary degeneration of cones (4). When $Pde6b^{STOP}/Pde6b^{H620Q}$ mice are crossed with a Cre transgenic line, the STOP cassette is removed and PDE6b is expressed in cells where Cre is expressed (5). We used two different Cre drivers to control the pattern and/or number of rescued rods. The first driver, *Pax6α::Cre*, encodes Cre recombinase under the control of a retina-specific regulatory element (α) of murine *Pax6*, a transcription factor expressed in retinal progenitor cells that gives rise to cells in distal retina (6). The second driver, *Pde6g::CreERT2*, is tamoxifen-inducible and encodes Cre recombinase under the control of the rod-specific

Significance

Retinitis pigmentosa is the leading cause of inherited blindness. Although gene therapy has the capacity to rescue diseased cells (usually rods), current methods generate retinas that are a mix of treated, rescued and untreated, dying rods. To determine whether the dying rods negatively impact rescue, we developed mouse models that allowed us to treat defined fractions of diseased rods. We found that dying rods did not trigger the death of rescued photoreceptors, even when the rescued cells are greatly outnumbered. On the other hand, the rescued photoreceptors did exhibit long-term defects, which were less severe when more rods were treated. Thus, although genetic rescue leads to survival of treated rods, it does not prevent other aspects of the retinitis pigmentosa pathology.

Author contributions: S.F.K. and S.H.T. designed research; S.F.K., C.-W.H., Y.-T.T., and C.-S.L. performed research; S.F.K., J.K.D., C.A.W.-S., and S.H.T. analyzed data; and S.F.K. and S.H.T. wrote the paper.

The authors declare no conflict of interest.

This article is a PNAS Direct Submission. R.R.M. is a guest editor invited by the Editorial Board.

[1]To whom correspondence should be addressed. Email: sht2@columbia.edu.

This article contains supporting information online at www.pnas.org/lookup/suppl/doi:10.1073/pnas.1615394114/-/DCSupplemental.

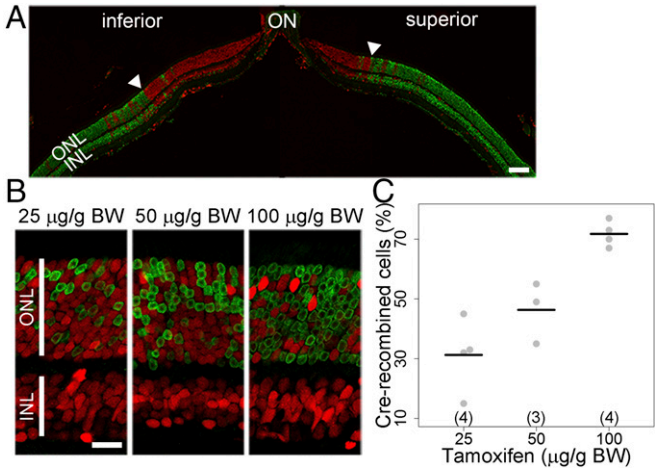

Fig. 1. Strategies for generating spatially and numerically reproducible mosaic patterns of rod rescue using two different Cre drivers. (*A*) Two-color fluorescent *ROSA*$^{nT\text{-}nG}$, *Pax6α::Cre* mice generated by crossing *Pax6α-Cre* and *ROSA*$^{nT\text{-}nG}$-reporter mice. Representative composite image of a retina from a 3-mo-old mouse, sectioned through the ON and immunolabeled for GFP (green, Cre-recombined cells). Arrowheads demark the border between predominantly nonrecombined and recombined areas. (*B*) Two-color fluorescent *ROSA*$^{nT\text{-}nG}$, *Pde6gCre::ERT2* mice generated by crossing *Pde6g::CreERT2* and *ROSA*$^{nT\text{-}nG}$-reporter mice; 1-mo-old mice were injected with 25, 50, or 100 µg/g BW tamoxifen; 2 wk later, retinas were sectioned and GFP immunolabeled. (*C*) Number of green and red nuclei was counted in a 90 × 90 µm area. *y* axis, total green nuclei divided by red + green nuclei; gray dots, individual mice (*n* values indicated on x axis); horizontal black lines, group means; red, tomato-fluorescence (nonrecombined cells). INL, inner nuclear layer; ON, optic nerve; ONL, outer nuclear layer. [Scale bars, 100 µm (*A*) and 15 µm (*B*).]

promoter of *Pde6g*, which encodes the gamma subunit of rod cGMP phosphodiesterase (5).

To define the patterns of *Pax6α::Cre* and *Pde6g::CreERT2* recombinase activity, we crossed our Cre transgenic lines with the *ROSA*$^{nT\text{-}nG}$ reporter mouse line. *ROSA*$^{nT\text{-}nG}$ mice contain a fluorescent allele that expresses nuclear-localized red fluorescence (tdTomato) in all cells, except those exposed to Cre recombinase; the latter cells express nuclear-localized enhanced green fluorescent protein (EGFP) (7). In *ROSA*$^{nT\text{-}nG}$, *Pax6α::Cre* flat-mounted retinas and sections from 3-mo-old mice, Cre-recombined cells (green) were detected predominantly in the distal retina (Fig. S1*A* and Fig. 1*A*); in flat-mounted retinas (n = 9), the green, Cre-recombined area was about 63 ± 1.3% (Fig. S1*B*), and in sections (n = 4 retinas) it started around 415 ± 30 µm (superior) and 675 ± 51 µm (inferior) from the optic nerve (Fig. 1*A*). Because the border between recombined and nonrecombined areas is not sharp (Fig. 1*A*, arrowheads), we defined it as the point at which the overwhelming majority of cells located more centrally were red (nonrecombined). In *ROSA*$^{nT\text{-}nG}$, *Pde6g::CreERT2* mice, red and green nuclei were uniformly distributed over the entire photoreceptor cell body-containing outer nuclear layer (ONL). As expected, only red nuclei were found in the inner nuclear layer (INL), which does not contain photoreceptor cell bodies (Fig. 1*B*)—and all cone nuclei were red (Fig. S2), because the *Pde6g::CreERT2* driver is only active in rods. The mean percentages of green Cre-recombined rod nuclei in the *ROSA*$^{nT\text{-}nG}$, *Pde6g::CreERT2* mice injected with tamoxifen at 25, 50, or 100 µg/g body weight (BW) were 31% ± 6, 46% ± 6, and 72% ± 2, respectively (i.e., roughly 30%, 50%, and 70%) (Fig. 1*C*). Thus, *Pde6g::CreERT2* activity can be controlled in vivo, albeit with variation, to achieve defined percentages of rods with allelic conversion.

Rescued Photoreceptors Appear to Migrate into Untreated Zones and Exhibit OS Shortening That Is More Dramatic the Farther the Migration. *ROSA*$^{nT\text{-}nG}$, *Pax6α::Cre* reporter mice have retinas with large, roughly segregated zones of recombined and nonrecombined cells (Fig. 1*A*). A single subretinal injection of gene therapy vectors (in both animals and humans) tends to yield a similar pattern of rescued and nonrescued cell zones. We therefore crossed *Pde6b*^{STOP}/*Pde6b*^{H620Q} and *Pax6α::Cre* mice to generate retinas with the same pattern seen in Fig. 1*A* and used PDE6b immunolabeling (rod OSs) to visualize areas with rescued rods. In retinas from 11-mo-old *Pde6b*^{STOP}/*Pde6b*^{H620Q}, Pax6α::*Cre* mice, immunolabeling was absent around the optic nerve—extending 138 ± 35 µm and 224 ± 47 µm in the superior and inferior directions, respectively (n = 3 retinas) (Fig. 2*A*); that is, the immunonegative zone was much smaller than the red nonrecombined zone (see Fig. 1*A* and associated text). Thus, at 11 mo, PDE6b expression was much closer to the optic nerve, suggesting that rescued rods may migrate into the untreated zone, but this hypothesis remains to be investigated. To assess retinal morphology in *Pde6b*^{STOP}/*Pde6b*^{H620Q}, Pax6α::*Cre* mice—in comparison with wild-type (*Pde6b*$^{+}$/*Pde6b*^{H620Q}) and mutant (*Pde6b*^{STOP}/*Pde6b*^{H620Q}) mice—retinal sections from 11-mo-old mice were stained with PDE6b antibody (rod OSs), PNA lectin (cone OS—as well as cone synapses), and Hoechst dye (nuclei) (Fig. S3*A*). In mutant retinas, ONL was almost gone due to photoreceptor cell loss, and PDE6b-labeled rod OSs and PNA-labeled cone OSs were completely absent. In *Pde6b*^{STOP}/*Pde6b*^{H620Q}, *Pax6α::Cre* retinas, untreated, PDE6b-negative areas were indistinguishable from mutant retinas, except that the former exhibited some PNA staining; treated areas were indistinguishable from wild-type retinas. In the most central part of the PDE6b-positive zone (i.e., bordering the PDE6b-negative zone), ONL

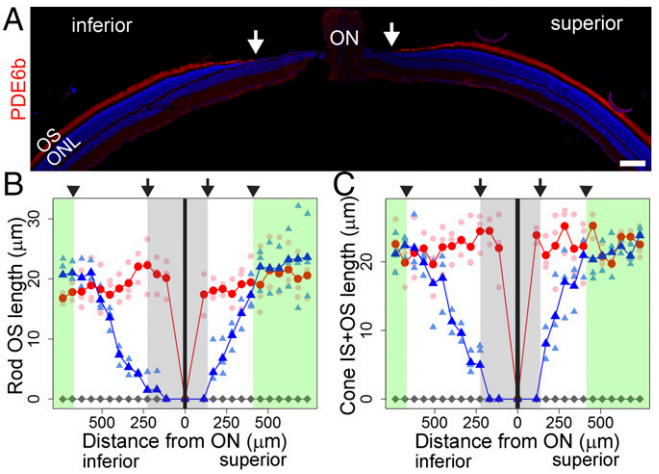

Fig. 2. Sustained shortening of rod and cone OSs, even after the period of rod cell death. (*A*) Retinal section (composite) from an 11-mo-old *Pde6b*^{STOP}/*Pde6b*^{H620Q}, *Pax6α::Cre* mouse immunolabeled for PDE6b (red, rod OSs) and stained with Hoechst dye (blue, nuclei). (*B* and *C*) Rod OS lengths and cone IS + OS lengths were measured in 11-mo-old retinal sections from wild-type (red circles), mutant (gray diamonds), and *Pde6b*^{STOP}/*Pde6b*^{H620Q}, *Pax6α::Cre* mice (blue triangles). Treated zones, green bars; untreated zones, white and gray bars. The border between treated and untreated zones (arrowheads here and in Fig. 1*A*) was measured in sections from *ROSA*$^{nT\text{-}nG}$, *Pax6α::Cre* mice (as in Fig. 1*A*; n = 4 mice). PDE6b-negative zone (gray bar) was measured in 11-mo-old sections from *Pde6b*^{STOP}/*Pde6b*^{H620Q}, *Pax6α::Cre* mice (as in *A*). Arrows in *A*–*C* demark the outer, peripheral border of the PDE6b-negative zone; bold symbols, group means; lighter colored symbols, individual mice (n = 3, for every group). Each line connects the group means. Black vertical line, optic nerve. IS, inner segment; ON, optic nerve; ONL, outer nuclear layer; OS, outer segment. (Scale bar, 100 µm.)

thickness and OS lengths were graded. We next quantified ONL thickness, cone number, rod OS length, and cone IS + OS length at multiple positions across a 1,500-μm length of the central retina (less than half of the area shown in Fig. 2*A*); identical quantifications were performed in wild-type and mutant retinas. In the PDE6b-negative area (gray bar in Fig. 2 *B* and *C* and Fig. S3 *B* and *C*), ONL thickness, rod OS length, and cone IS + OS length were not significantly different from mutant retinas; however, cone number was significantly increased ($P < 0.01$). In the area just outside the PDE6b-negative zone (white bars in Fig. 2 *B* and *C* and Fig. S3 *B* and *C*), ONL thickness and OS length were graded (values decreased as the distance to the PDE6b-negative zone decreased). The graded ONL appears to be mainly the result of treated photoreceptors moving into untreated areas, but there may be alternative explanations (Fig. S3 *B* and *C*; note blue triangles in white bars). On the other hand, the graded OS lengths in these 11-mo retinas (by which time, diseased rods have all died) suggest that some unknown pathological feature(s), other than dying rods, sustains the shortened OS phenotype. Finally, in treated areas (green bars in Fig. 2 *B* and *C* and Fig. S3 *B* and *C*), all four features were not significantly different from wild-type retinas, demonstrating that rescued rods and cones were not negatively impacted by distant degenerating rods. On the other hand, the increased numbers of cones in untreated areas might result from migration of rescued cones from treated areas (*Discussion*).

Treated Rods, Cones, and Their OSs Are All Rescued in a Dose-Dependent Fashion. Using our *ROSA*$^{nT\text{-}nG}$, *Pde6g::CreERT2* reporter mice, we demonstrated that the percentage of recombined rods can be controlled by the tamoxifen dose (Fig. 1 *B* and *C*). We therefore crossed *Pde6b*^{STOP}/*Pde6b*^{H620Q} and *Pde6g::CreERT2* mice to generate RP mice with the same degree of dose–response control. To verify that PDE6b expression correlates with tamoxifen dose, we injected tamoxifen in 19-d-old *Pde6b*^{STOP}/*Pde6b*^{H620Q}, *Pde6g::CreERT2* mice (i.e., before photoreceptor degeneration) (5) and then performed immunoblot analysis on retinas when the mice were 12 wk old. PDE6b expression was, in fact, proportional to tamoxifen dose (Fig. S4).

To mimic RP gene therapy at midstage disease, 1-mo-old *Pde6b*^{STOP}/*Pde6b*^{H620Q}, *Pde6g::CreERT2* mice, which have lost roughly 30% of their rods (5), were injected with 25, 50, or 100 μg/g BW tamoxifen (i.e., low-, medium-, and high-efficiency genetic rescue). We demonstrated (Fig. 1*C*) that these three doses rescue ∼30%, 50%, and 70% of the remaining rods. Therefore, our treatment rescued ∼20%, 35%, or 50% of the total, original rods. To analyze the effects of this treatment on retinal structure, retinas from 9-mo-old mice were sectioned and immunolabeled. To distinguish rods and cones, we immunolabeled sections with rhodopsin antibody (rod OSs) and arrestin antibody (cones) (Fig. 3*A*, *Top*). In treated retinas, there was clear dose-dependent rescue of rhodopsin-positive rod OSs and the ONL. In addition, the arrestin immunolabeling revealed dramatic dose-dependent rescue of cones—especially cone OS length. The small amount of arrestin immunolabeling in mutant retinas represents the fraction of cone cells—devoid of their OSs—that persist for some time after mutant rods have died (8).

The OSs of treated retinas exhibited PDE6b immunolabeling (Fig. 3*A*, *Bottom*)—thereby demonstrating survival of treated rods. Further, we performed PCR analysis on DNA isolated from the retinal ONL. A 415-bp band was found in DNA amplified from mutant mice but not in DNA amplified from treated mutant ONL (Fig. S5). The removal of the STOP cassette in treated rods leads to a shorter 362-bp band; therefore, all rods in the treated retinas were devoid of the STOP cassette.

To quantify photoreceptor rescue, we measured ONL thickness (rods + cones), cone numbers, rod OS length, and cone IS + OS length (Fig. 3*B*). All four structural measures were significantly greater in treated retinas, compared with untreated mutants ($P < 0.001$). ONL thickness, rod OS length, and cone IS + OS length were all significantly less than wild type ($P < 0.001$). ONL thickness was less than wild type because treatment was administered at 1 mo, when 30% of rods have already died, and because only 70% or less of the remaining rods were treated. Similarly, it is not surprising that rod OS and cone IS + OS lengths were not fully restored to wild-type lengths by 9 mo, given that the rescued photoreceptors inhabit a retina that has lost 50–80% of the original rods. In addition, rescue of ONL, rod

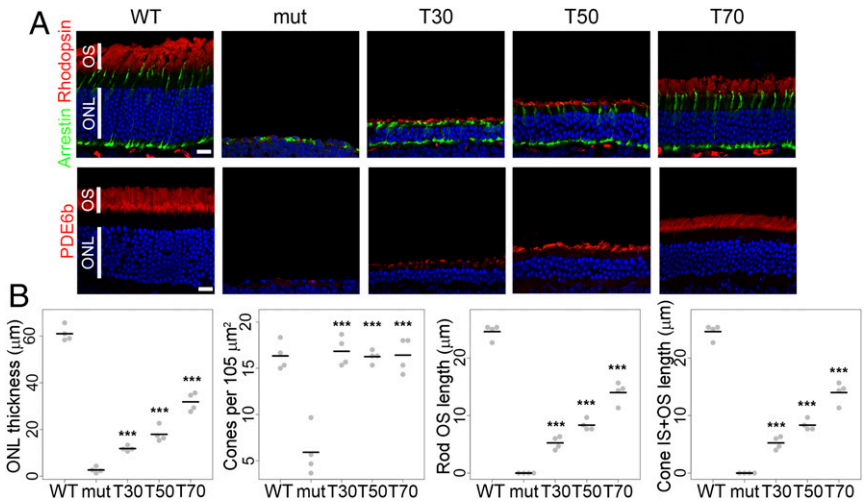

Fig. 3. Restoration of PDE6b expression rescues rods and partially restores OS length, in a dose-dependent fashion, and prevents cone death. *Pde6b*^{STOP}/*Pde6b*^{H620Q}, *Pde6g::CreERT2* mice were injected with 25, 50, or 100 μg/g BW tamoxifen to rescue 30% (T30), 50% (T50), or 70% (T70) of rods, respectively; untreated mutants (mut) and wild-type mice (*Pde6b*$^{+}$/*Pde6b*^{H620Q}, *Pde6g::CreERT2*, WT) were not injected. Tamoxifen injections were in 1-mo-old mice; at 9 mo of age, retinas were sectioned and immunolabeled. (*A*) Antibodies: rhodopsin or PDE6b (rod OSs, red) and arrestin (cones, green). Hoechst dye, nuclei, blue. Arrows, arrestin-immunopositive cone cell bodies; arrowheads, arrestin-immunopositive cone OSs. (*B*) Rhodopsin and arrestin immunolabeled sections were quantitatively analyzed for ONL thickness, cone number, rod OS length and cone IS + OS length. Gray dots, individual mice ($n = 4$ for each group); horizontal black lines, group means. Treated and untreated groups were compared by a linear regression model: ***$P < 0.001$. IS, inner segment; ONL, outer nuclear layer; OS, outer segment. (Scale bar, 15 μm.)

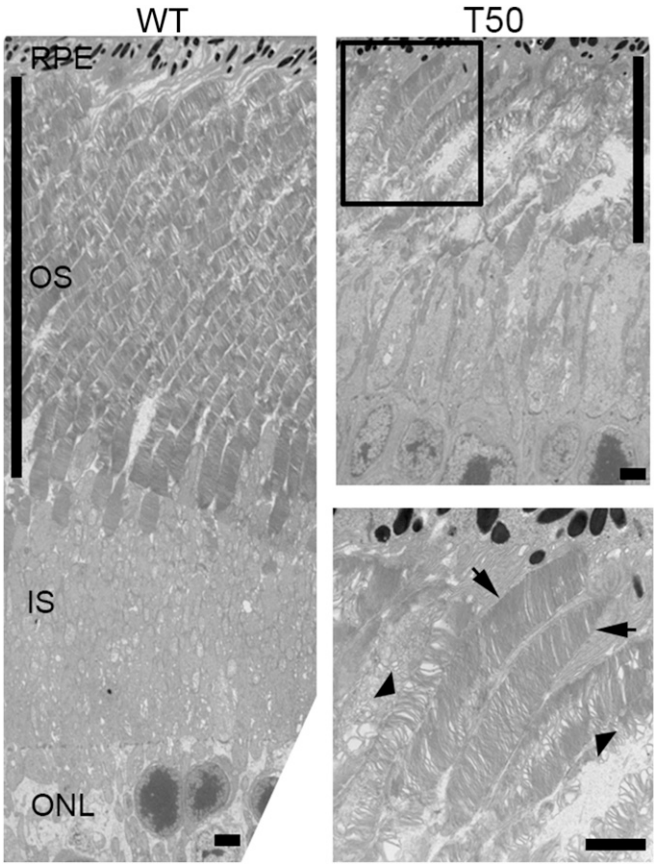

Fig. 4. Ultrastructural dysgenesis in OSs of rescued retinas. *Pde6b*^{STOP}/*Pde6b*^{H620Q}, *Pde6g::CreERT2* mice were injected with 50 μg/g BW tamoxifen to rescue 50% (T50) of rods, respectively; wild-type mice (*Pde6b*$^{+}$/*Pde6b*^{H620Q}, *Pde6g::CreERT2*, WT) were not injected. Tamoxifen injections were in 1-mo-old mice; at 8 mo of age, retinas were sectioned and processed for electron microscopy. Wt is a composite image. Arrows, normal OSs; arrowheads, disrupted OSs; vertical black bars, approximate OS length. IS, inner segment; ONL, outer nuclear layer; OS, outer segment. RPE, retinal pigment epithelium. (Scale bar, 2 μm.)

OS, and (for the most part) cone IS + OS length were dose-dependent: 70% rod-rescued retinas vs. 50% or 30% ($P < 0.001$); ONL thickness and rod OS length in T50 vs. T30 ($P < 0.003$ and $P < 0.008$, respectively). Importantly, in all treated retinas, even in those in which only 30% of remaining rods were rescued, cone numbers were not significantly different from wild type ($P = 0.7$, 0.9 and 0.9, respectively). In summary, our gene-rescue strategy in midstage disease mice led to the dose-dependent structural rescue of rods and prevented non-cell autonomous cone death.

Rescued OSs Are Dysmorphic—Even After the Phase of Rod Death. To further assess structural changes in OSs, 1-mo-old *Pde6b*^{STOP}/*Pde6b*^{H620Q}, *Pde6g::CreERT2* mice were tamoxifen-injected (or not), and at 8 mo, retinas were analyzed by light and electron microscopy. Light microscopy of H&E stained sections (Fig. S6*A*) showed normal OSs in wild-type retinas, no OSs in untreated mutants, and rescued OSs in treated retinas. As shown in Fig. 3, rescue of the OS length was clearly dose-dependent and partial. The dose-dependent shortening of OSs was confirmed in electron micrographs of treated retinas (Fig. 4 and Fig. S6*B*). In addition, in the T50 retinas, we noted holes in the OS layer and that the OSs were no longer arranged in cohesive linear arrays. Further, in some OSs, the membranous discs appeared disrupted (Fig. 4, detail). Although such changes are sometimes seen in wild-type EM images, we noted a clear dose dependence to the ultrastructural phenotype; although all retinas were processed at the same time, only the T50 retinas displayed the pronounced abnormality.

Rod and Cone Function Are Rescued, and That Rescue Is Dose-Dependent. To determine if retinal function was rescued, 1-mo-old *Pde6b*^{STOP}/*Pde6b*^{H620Q}, *Pde6g::CreERT2* mice were tamoxifen injected (or not), and 8 mo later, electroretinography (ERG) analysis was performed. To derive mixed rod and cone ERG responses, mice were dark-adapted and then eyes were exposed to bright flashes. Wild-type retinas exhibited a photoreceptor-mediated a-wave (negative deflection) followed by an inner retina-mediated b-wave (positive deflection). In contrast, untreated mutant retinas lacked the a-wave and exhibited a strongly reduced b-wave. Treatment rescued the a- and b-waves (Fig. 5 *A* and *B*); as expected, rescue was not to wild-type levels, as treatment was administered at 1 mo, when about 30% of rods had already died and 70% or fewer of the remaining rods were treated (i.e., ~50% or fewer of the total/original rods). In mutant retinas in which 50% and 70% of the remaining rods were rescued (and shown in Fig. 3*C* to be significantly different), functional rescue was not significantly different (a-waves, $P = 0.8$; b-waves, $P = 0.7$). This suggests that the relationship between structural and functional rescue is nonlinear and/or that the variability in a- and b-wave amplitudes may decrease the ability to detect subtle differences. In these T50 and T70 retinas, a- and b-wave amplitudes were significantly greater than either untreated mutant retinas ($P < 0.001$) or T30 retinas (T50, $P < 0.003$ and 0.002, respectively; T70, $P < 0.001$). In T30 retinas, b-wave amplitudes were significantly greater than untreated mutants ($P < 0.001$), but a-wave amplitudes were not ($P = 0.1$).

Analysis of Disease Progression in Mosaic Retinas Suggests Non-Cell Autonomous Triggers of OS Dystrophy and Cell-Autonomous Triggers of Rod Death. To understand disease progression in our rescued mosaic retinas, 1-mo-old *Pde6b*^{STOP}/*Pde6b*^{H620Q}, *Pde6g-CreERT2*

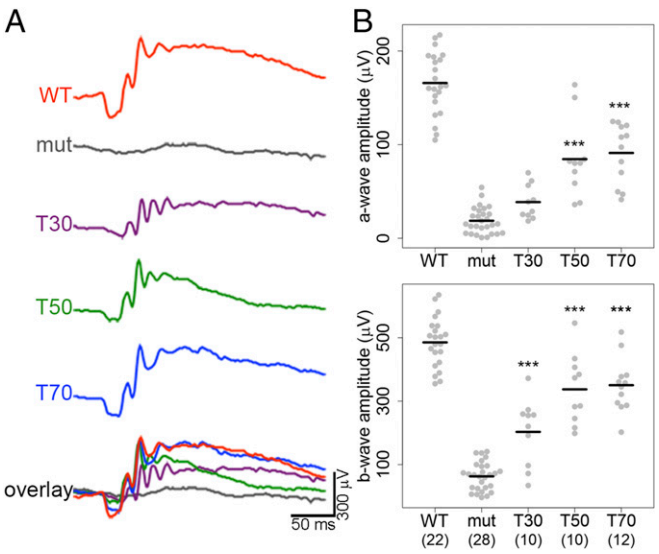

Fig. 5. Rescue of photoreceptor function is proportional to the number of treated rods. *Pde6b*^{STOP}/*Pde6b*^{H620Q}, *Pde6g::CreERT2* mice were injected with 25, 50, or 100 μg/g BW tamoxifen to rescue 30% (T30), 50% (T50), or 70% (T70) of rods, respectively; untreated mutants (mut) and wild-type mice (*Pde6b*$^{+}$/*Pde6b*^{H620Q}, *Pde6g::CreERT2*, WT) were not injected. Tamoxifen injections were in 1-mo-old mice; at 9 mo of age, retinal function was analyzed by ERG. (*A*) Representative ERG responses. (*B*) Quantification of ERG a-wave and b-wave amplitudes. Gray dots, individual eyes (*n* values indicated on *x* axis); horizontal black lines, group means. Treated and untreated groups were compared using a linear mixed model: ***$P < 0.001$.

mice were tamoxifen injected (or not), and photoreceptor layer structural features were measured at 1, 2.5, 5, and 9 mo of age (Fig. 6 and Fig. S7). In wild-type retinas, photoreceptor layer features were stable over the 8-mo study: ONL thickness, $P = 0.9$; rod OS length, $P = 0.5$; cone IS + OS length, $P = 0.5$ (P values are for 1 vs. 9 mo). In contrast, untreated, mutant retinas exhibited progressive and dramatic thinning of the ONL ($P < 0.001$) and shortening of both rod and cone OSs ($P < 0.001$). T30 and T50 retinas also exhibited significant decreases in ONL thickness ($P < 0.006$) but only over the first 4 mo; there was no significant change over the last 4 mo ($P = 0.9$ and 0.5 for T30 and T50, respectively) (Fig. 6). T70 retinas exhibited a modest decrease in ONL thickness over the first 4 mo that was not significant ($P = 0.09$). Thus, in treated mutants, the only significant decrease in ONL thickness was in retinas from mice treated at the two lower doses and only for the first 4 mo following treatment. If this decrease is due entirely to cell-autonomous death of untreated rods, then we would predict stable survival of all of the treated rods (i.e., 31%, 46%, and 72% of *remaining* rods for the three tamoxifen doses, respectively; Fig. 1*C*). In fact, at 9 mo, actual rod survival values were 31%, 46%, and 82%, which are not significantly different from the predicted values ($P = 0.6$, 0.9, and 0.3, respectively). Cones were not taken into account, as they make up only 3% of photoreceptors in normal retinas (9). Thus, these data provide indirect evidence for the stable, sustained survival of the vast majority of (if not all) treated rods in a diseased environment. We found that the overall dose-dependent pattern of OS shortening over the 8-mo timeframe was the same as ONL thickness (Fig. S7 and Fig. 6, respectively). For T30 and T50 retinas, rod and cone OS length decreased significantly over the first 4 mo ($P < 0.05$) but not over the last 4 (Fig. S7 *A* and *B*, respectively). For T70 retinas, there was no significant change in either rod OS or cone IS + OS lengths over the 8-mo period ($P = 0.7$ and 0.5, respectively). These data suggest that in treated retinas, rod and cone OSs progressively shorten until most, if not all, untreated mutant rods have died (around 5 mo). This, in turn, implies that OS shortening is driven by non-cell autonomous mechanisms, triggered by dying untreated rods.

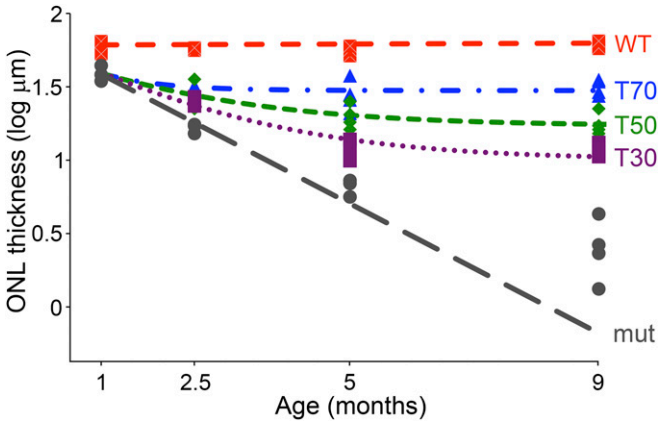

Fig. 6. Dying rods do not diminish the long-term survival of neighboring rescued rods. *Pde6b*^{STOP}/*Pde6b*^{H620Q}, *Pde6g::CreERT2* mice were injected with 25, 50, or 100 µg/g BW tamoxifen to rescue 30% (T30), 50% (T50), or 70% (T70) of rods, respectively; untreated mutants (mut) and wild-type mice (*Pde6b*$^{+}$/*Pde6b*^{H620Q}, *Pde6g::CreERT2*, WT) were not injected. Tamoxifen injections were in 1-mo-old mice. Wild-type and untreated mutant mice were killed at 1, 2.5, 5, and 9 mo; treated mice were killed at 2.5, 5, and 9 mo (9-mo data are also shown in Fig. 3). Each symbol represents an individual mouse; $n = 4$ for all genotypes and/or treatments and time points, except $n = 3$ for untreated mutants at 1 mo and for all groups at 2.5 mo. Mutant mice were fitted to an exponential decay model; treated mice were fitted to an exponential decay model with plateau (see Eq. **S1** in *SI Materials and Methods*).

Discussion

In RP, degeneration and, subsequently, death of diseased, mutant rods leads to the non-cell autonomous loss of wild-type cones (2, 10, 11). However, it is not known if degenerating rods have non-cell autonomous effects on the rods surrounding them. This issue is most relevant in gene therapy-treated retinas—in terms of understanding whether rescued rods are negatively impacted by untreated rods. To study this, we used two different Cre drivers to express a therapeutic gene in diseased rods in a mouse model of RP. One driver, *Pax6α::Cre*, yielded retinas in which treated and untreated rods were roughly segregated, thereby modeling human gene therapy-treated retinas. The second driver, *Pde6g::CreERT2*, generated retinas in which rescued rods were diffusely distributed over the entire photoreceptor layer (i.e., treated and untreated rods were intermixed), and importantly, the percentage of rescued rods was controlled. In both mice, we did not restore the mutant gene in *all* diseased rods, as we have done before (5). Data from these two distinct recombinant retinas strongly suggest that rod rescue is stable, even when the vast majority of rods are untreated (i.e., mutant). The findings from this study and a previous one (5) support two of the major predictions of the "one-hit" model of cell death (12): (*i*) rod photoreceptor death is cell-autonomous (this study), and (*ii*) mutant photoreceptors can be rescued even when the activity of the relevant gene is restored at late-stage disease (5).

Although our quantitative analysis suggests that few, if any, rescued rods died, we did observe nonlethal phenotypes in surviving photoreceptors. Specifically, where dying and rescued photoreceptors were intermixed, rod and cone OSs were shortened. Although the highest efficiency treatment (70% rescue of remaining rods and 50% rescue of total rods) in *Pde6b*^{H620Q}/*Pde6b*^{STOP}, *Pde6g::CreERT2* mice halted the shortening, OSs in the lower efficiency rescued retinas (50% and 30% rescue of remaining rods and 35% and 21% of total rods, respectively) continued to shorten but then plateaued at the same time as ONL thickness (i.e., when most untreated rods have died). These dose–response disease-progression data suggest that OS shortening is triggered non-cell autonomously by dying mutant rods, and only manifests when there is a preponderance of dying rods. Indeed, OS shortening was not apparent within rescued zones in our *Pax6α::Cre* retinas. Thus, OS shortening might not occur within rescued regions of treated human RP retina.

The finding that shortened OSs do not regrow to their normal length indicates a shift in the homeostasis between OS morphogenesis and retinal pigment epithelial (RPE) cell phagocytosis (13, 14). Under favorable conditions, rod and cone OSs are capable of regrowth—for example, following light-induced damage (15), retinal detachment (16), or macular hole surgery (17). However, the extent and time course of regrowth depend on the severity of the damage (15). For example, retinal genetic rescue at advanced disease stages does not lead to OS regeneration (5, 18, 19), suggesting a correlation between photoreceptor numbers and OS synthesis. Perhaps a critical number of rods might be needed to release glucose from RPE, where it is sequestered following rod degeneration and thus unavailable to support OS synthesis (8, 20). Interestingly, in untreated RP patients (and mice), the earliest detected histopathologic change is rod OS dysgenesis. Our data demonstrate that OS dysgenesis does not, by itself, necessarily trigger cell death. This suggests that OS dysgenesis and cell death are phenotypes of two separate pathogenesis pathways.

Our experiments, which were designed to study the fate of rescued rods in a diseased environment, strongly suggest that survival of rescued rods is not affected by dying, untreated rods. Two previous mouse studies came to the opposite conclusion

(21–23). In one of those studies (21), retinas from a total of three aggregation chimeras expressing mutant pig rhodopsin were shown to have 7%, 16%, or 42% normal rods distributed in patches. ONL thickness in the 42% of rescued retinas was relatively uniform and intermediate between wild-type and predominantly transgenic retinas. The second study (22) examined hemizygous-transgenic female mice on a retinal degeneration slow ($rds^{-/-}$) background (transgene present on only one X-chromosome); in situ hybridization revealed a mosaic pattern of transgene expression (rescue) in retinas, and ONL thickness was uniform in 2-mo-old hemizygous females. In both studies, the authors expected to see nonuniform ONL—rescued patches with normal thickness ONL, alternating with mutant patches of thin ONL. However, data from both of our mutants strongly suggest that surviving photoreceptors undergo active or passive rearrangement in response to the dramatic physical changes to the photoreceptor layer landscape—essentially filling in the void left by degenerating rods to yield an ONL that is either uniform in thickness ($Pde6b^{H620Q}/Pde6b^{STOP}$, *Pde6g::CreERT2* mutant) or graded ($Pde6b^{H620Q}/Pde6b^{STOP}$, *Pax6α::Cre* mutant). In fact, remodeling of photoreceptor cells has been observed in a canine model of X-linked RP (*XLPRA2*); these diseased retinas exhibit patches of diseased and normal retina, which gradually disappear over time (24). In addition, retinas from chimeric mice (produced by combining morulae from $rds^{-/-}$ and wild-type mice) showed regions with normal, intermediate, and thin ONL thickness (25). On the other hand, the cell autonomy of rod death may not be generalizable to all rod degenerations.

Our experiments model three features of human gene therapy-treated retinas. First, like gene therapy-treated retinas, our mouse retinas are mosaics of rescued and unrescued rods. Second, because patients are typically diagnosed after onset of degeneration, we treated our $Pde6b^{H620Q}/Pde6b^{STOP}$, *Pde6g::CreERT2* mice when roughly 30% of rods had already died. Third, the typical single subretinal injection is restricted to a small area, resulting in large swaths of untreated cells—much like our $Pde6b^{H620Q}/Pde6b^{STOP}$, *Pax6α::Cre* mice. Our mouse data suggest that in gene therapy-treated RP patients, improvement of visual function would be stable, cone death would be halted in treated regions, and OS shortening would only be in a narrow zone bordering the treated areas. However, if our findings do not fully translate to human RP, it could be because our genetic rescue is based on allelic conversion (i.e., the "wild-type" sequence of the PDE6b gene is restored). In contrast, the AAV-mediated gene replacement therapy currently favored in patients may not yield physiological levels of protein production—although mouse studies suggest otherwise (26). In addition, our results may or may not apply to all types of inherited retinal degeneration, given their diverse etiologies (27).

Our mouse data from this study and a previous one (5) demonstrate that correction of the genetic defect is sufficient to prevent death in treated rods and that the extent of rescue depends on the number of treated rods (more is better) and the timing of treatment (earlier is better).

Materials and Methods

All experiments were approved by the Institutional Animal Care and Use Committee (IACUC) at Columbia University. Methods are detailed in *SI Materials and Methods*.

ACKNOWLEDGMENTS. We thank Richard Davis and members of the Jonas Stem Cell and Brown Glaucoma Laboratories for sharing ideas and equipment. We also thank Rebecca Tuttle for critically reviewing the manuscript. C.A.W.-S. is funded by the German Research Council (DFG, SFB870). S.H.T. is a member of the RD-CURE Consortium and is supported by the Tistou and Charlotte Kerstan Foundation; NIH Grants R01EY018213, R01EY024698, R01EY026682, and R21AG050437; a Research to Prevent Blindness (RPB) Physician-Scientist Award; the Schneeweiss Stem Cell Fund; New York State (N09G-302 and N13G-275); Foundation Fighting Blindness New York Regional Research Center Grant C-NY05-0705-0312; Kobi and Nancy Karp; the Crowley Research Fund; the Gebroe Family Foundation; and Burroughs Welcome Career Awards in Biomedical Sciences Program. The Columbia Confocal and animal facilities are supported by NIH Core Grants 5P30EY019007 and 5P30CA013696 and unrestricted funds from RPB and Columbia University.

1. Daiger SP, Sullivan LS, Bowne SJ (2013) Genes and mutations causing retinitis pigmentosa. *Clin Genet* 84:132–141.
2. Narayan DS, Wood JP, Chidlow G, Casson RJ (2016) A review of the mechanisms of cone degeneration in retinitis pigmentosa. *Acta Ophthalmol* 94:748–754.
3. Shen S, Sujirakul T, Tsang SH (2014) Next-generation sequencing revealed a novel mutation in the gene encoding the beta subunit of rod phosphodiesterase. *Ophthalmic Genet* 35:142–150.
4. Davis RJ, et al. (2013) Therapeutic margins in a novel preclinical model of retinitis pigmentosa. *J Neurosci* 33:13475–13483.
5. Koch SF, et al. (2015) Halting progressive neurodegeneration in advanced retinitis pigmentosa. *J Clin Invest* 125:3704–3713.
6. Marquardt T, et al. (2001) Pax6 is required for the multipotent state of retinal progenitor cells. *Cell* 105:43–55.
7. Prigge JR, et al. (2013) Nuclear double-fluorescent reporter for in vivo and ex vivo analyses of biological transitions in mouse nuclei. *Mammalian Genome* 24:389–399.
8. Wang W, et al. (2016) Two-step reactivation of dormant cones in retinitis pigmentosa. *Cell Reports* 15:372–385.
9. Applebury ML, et al. (2000) The murine cone photoreceptor: A single cone type expresses both S and M opsins with retinal spatial patterning. *Neuron* 27:513–523.
10. Aït-Ali N, et al. (2015) Rod-derived cone viability factor promotes cone survival by stimulating aerobic glycolysis. *Cell* 161:817–832.
11. Xiong W, MacColl Garfinkel AE, Li Y, Benowitz LI, Cepko CL (2015) NRF2 promotes neuronal survival in neurodegeneration and acute nerve damage. *J Clin Invest* 125: 1433–1445.
12. Clarke G, et al. (2000) A one-hit model of cell death in inherited neuronal degenerations. *Nature* 406:195–199.
13. Young RW (1976) Visual cells and the concept of renewal. *Invest Ophthalmol Vis Sci* 15:700–725.
14. Clarke G, et al. (2000) Rom-1 is required for rod photoreceptor viability and the regulation of disk morphogenesis. *Nat Genet* 25:67–73.
15. Rapp LM, Fisher PL, Dhindsa HS (1994) Reduced rate of rod outer segment disk synthesis in photoreceptor cells recovering from UVA light damage. *Invest Ophthalmol Vis Sci* 35:3540–3548.
16. Guérin CJ, Lewis GP, Fisher SK, Anderson DH (1993) Recovery of photoreceptor outer segment length and analysis of membrane assembly rates in regenerating primate photoreceptor outer segments. *Invest Ophthalmol Vis Sci* 34:175–183.
17. Mitamura Y, et al. (2013) Photoreceptor impairment and restoration on optical coherence tomographic image. *J Ophthalmol* 2013:518170.
18. Beltran WA, et al. (2015) Successful arrest of photoreceptor and vision loss expands the therapeutic window of retinal gene therapy to later stages of disease. *Proc Natl Acad Sci USA* 112:E5844–E5853.
19. Sarra GM, et al. (2001) Gene replacement therapy in the retinal degeneration slow (rds) mouse: The effect on retinal degeneration following partial transduction of the retina. *Hum Mol Genet* 10:2353–2361.
20. Zhang L, et al. (2016) Reprogramming metabolism by targeting sirtuin 6 attenuates retinal degeneration. *J Clin Invest* 126:4659–4673.
21. Huang PC, Gaitan AE, Hao Y, Petters RM, Wong F (1993) Cellular interactions implicated in the mechanism of photoreceptor degeneration in transgenic mice expressing a mutant rhodopsin gene. *Proc Natl Acad Sci USA* 90:8484–8488.
22. Kedzierski W, Bok D, Travis GH (1998) Non-cell-autonomous photoreceptor degeneration in rds mutant mice mosaic for expression of a rescue transgene. *J Neurosci* 18:4076–4082.
23. Rattner A, Sun H, Nathans J (1999) Molecular genetics of human retinal disease. *Annu Rev Genet* 33:89–131.
24. Beltran WA, Acland GM, Aguirre GD (2009) Age-dependent disease expression determines remodeling of the retinal mosaic in carriers of RPGR exon ORF15 mutations. *Invest Ophthalmol Vis Sci* 50:3985–3995.
25. Sanyal S, Zeilmaker GH (1984) Development and degeneration of retina in rds mutant mice: Light and electron microscopic observations in experimental chimaeras. *Exp Eye Res* 39:231–246.
26. Nishiguchi KM, et al. (2015) Gene therapy restores vision in rd1 mice after removal of a confounding mutation in Gpr179. *Nat Commun* 6:6006.
27. Hurley JB, Chao JR (2015) It's never too late to save a photoreceptor. *J Clin Invest* 125: 3424–3426.
28. Guo L, et al. (2014) Direct optic nerve sheath (DONS) application of Schwann cells prolongs retinal ganglion cell survival in vivo. *Cell Death Dis* 5:e1460.